The Generalized Plant Allometry that Advances Metabolic Ecology Theory

Stuart Bryce Dixon Sopp (s.sopp@bangor.ac.uk)
Bangor University https://orcid.org/0000-0002-0777-4493
Ruben Valbuena
Bangor University https://orcid.org/0000-0003-0493-7581

Research Article

Keywords: Metabolic Ecology Theory, Allometry, Tissue functionality, Height-diameter scaling

Posted Date: September 9th, 2021

DOI: https://doi.org/10.21203/rs.3.rs-871867/v1

Main Manuscript

Title: The Generalized Plant Allometry that Advances Metabolic Ecology Theory.

Authors: S.B.D. Sopp (1)*, and R. Valbuena (1)*

Affiliations:

(1) School of Natural Sciences, Bangor University, Bangor, LL57 2UW, UK

* **Corresponding authors:** s.sopp@bangor.ac.uk, r.valbuena@bangor.ac.uk

This file includes:

Abstract

Main text

References

Figures (1-5)

Tables (1 and 2)

Abstract

Plant allometry is key for determining the role of forests in global carbon cycles, through the calculation of tree biomass using proxy measurements such as tree diameters or heights. Metabolic ecology theory (MET) considers the general principles that underpin allometry, but MET scaling relationships have been challenged on their lack of fit to empirical data and global applicability. We postulated that MET scaling is applicable only for plant tissues combining conductive and supportive functionality (tracheids), but as plants evolved tissues of specialized conductive functionality (vessels) their allometry progressed into more complex relationships. According to this principle, we deducted generalized MET (gMET) relationships with mechanistically deducted coefficients. Our gMET models proved to have exceptional empirical support against global datasets, achieving unbiased predictions across biomes worldwide. These results prove gMET models to be a crucial improvement to MET-based allometry, providing a universally applicable theoretical framework for worldwide estimations of forest carbon.

Main text

Metabolic ecology theory (MET) provides a broad framework which sheds light upon scaling relationships within biological organisms[1,2], with implications for understanding ecosystem growth and dynamics[3], ecosystem structure[4-6], and to a greater extent net primary productivity and ecosystem energy and carbon cycles[7-9]. However, the plant allometric relationships derived through MET have faced criticism for their lack of empirical support, with larger trees particularly deviating from the predictions[10-12]. For this reason, there has been attempts to adjust its theoretical basis[13], such as the inclusion of additional aspects like canopy geometry packing dynamics[14,15] or the influence of asymmetric competition of larger trees for resources[16]. Despite these attempts, a single succinct mechanistic advancement, explaining the lack of fit to empirical data and resulting in a coherent set of allometric relationships, has not been realized.

Some of the key allometric equations that stem from MET provide scaling relationships between the diameter (d) of a plant and its height (h), volume or aboveground biomass (agb) and subsequently carbon. MET^2 dictates that the h an individual tree reaches scales to 2/3s of its d. However this h-d relationship often fits poorly to real tree data, with many studies fitting power laws notably below 2/3[11,17-19], with the greatest deviation shown by large trees which exhibit exponents significantly lower[20-22]. Consequently, the geometrically propagated agb-d exponent of 8/3 predicted by MET^2 is consistently higher than adjusted models worldwide[23-26]. Scholars have therefore taken to using model forms other than power laws that empirically suit their datasets[27-29], thereby preferring statistically optimised model forms, over theory-based models[17,30-31]. The question is therefore raised as to whether a suitable mechanistic model other than a simple

power relationship can be derived from MET, conciliating the current divide between theoretical and statistical plant allometry models.

To investigate the lack of theory-consistent scaling in empirical tree data, a re-evaluation of the underpinning assumptions for MET's allometry is needed, considering the conductive resistance and support requirements affecting plants as they grow in size[32]. Hydraulic and mechanical constraints are typically cited as key influences of plant allometry, with their interaction governing h[33]. A trade-off between these two constraints is evident[34], particularly for large trees[35,36]. Each constraint can be considered through the proportion of tissue with conductive (CT) and supportive (ST) functionality within a cross-section of the stem[37,38] (Fig. 1). At a cellular level, these functions manifest differently between species, as angiosperms contain vessels and fibres, respectively with distinct conductive and supportive roles, while gymnosperms typically have tracheids that integrate both functions[39].

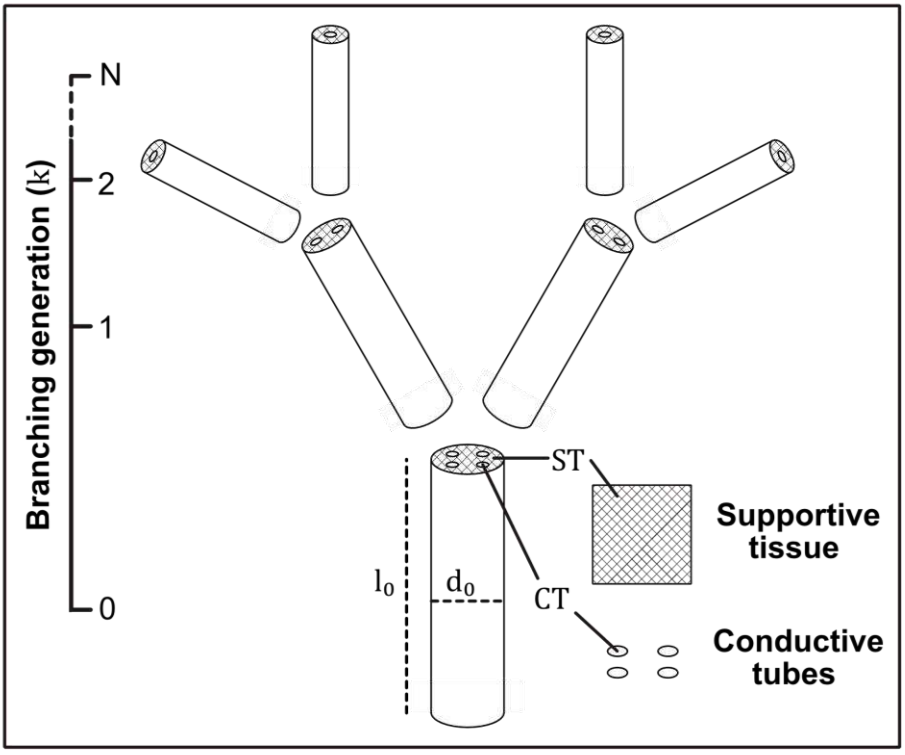

Fig. 1 | Tree architecture illustrating the differentiation of supportive and conductive systems within a branching network. This differentiation is set out by Eq. 9.

We postulated that a distinction between CT and ST is required to advance the current theory and overcome the shortfalls of the original MET scaling. We therefore revisited MET's underpinning assumptions and used them to derive a new set of allometric equations which consider the interaction between conductive and supportive functionality, integrating mechanical and hydraulic limitations into MET scaling. We hypothesized that this advancement would generate generalized MET (gMET) model forms for the h-d and agb-d relationships which would adequately fit vascular plants independently of functional type (angiosperm/gymnosperm) or geographical location (biome), clarifying the reasons for the apparent lack of empirical fit in large trees and for certain tree species. We show that the theoretical gMET equations demonstrate statistical and conceptual validity globally, and better statistical models that are widely used as the gold standard for estimating biomass carbon in tropical forests[27]. Most importantly, these results substantiate that the implications of MET in plant allometry hold true globally.

Rationale for the generalized MET (gMET) model

The 2/3 scaling relationship between d and h predicted by MET derives strictly from biomechanical limitations of an area-preserving and volume filling network of branching geometry[2,33,39-40]. The original formulation of allometry derived from MET assumes that the biomechanical capabilities of both CT and ST are equivalent to derive the 2/3 exponent in the $h \propto d^{2/3}$ scaling[1,2]. Plant xylem is however not functionally designed for structural support, since it maximizes conductance (Murray's law)[42,43]. Consequently, we assume that ST is solely responsible for the supportive functionality. Our models are therefore underpinned by the postulate that the 2/3 scaling relationship should be applied

exclusively to ST (see Methods). Accordingly, we propose a modification of the original MET h-d scaling relationship, which has subsequent implications for other allometric laws derived from MET, such as the agb-d scaling.

The development of our generalized h-d relationship stems from another MET-derived scaling law[2] which dictates that the proportion of tissue with conductive function scales to the diameter as $CT \propto d^{1/3}$. This implies that CT rises to overcome hydraulic constraints as a tree grows, and thus the proportion of non-lumen tissue with supportive functionality $ST = 1 - CT$ decreases with diameter[35,44]. Despite this reduction in ST, the net mechanical strength continues to increase with tree diameter, as the resistance generated by fibres increases with distance from a neutral axis[45]. Thus, the empirical evidence that growth in height slows in larger trees[20-22] can be explained under the consideration that the 2/3 scaling only concerns to the proportion of tissue with supportive functionality $h \propto (STd)^{2/3}$ (see Eq. 9 in Methods). A component of decrease in ST can thus be included, effectively modelling the dynamic interaction between the two tissue types that govern the hydraulic and mechanical constraints to tree growth.

Applying this modification of the original MET scaling laws gives the generalized gMET h-d allometric equation (see Methods for full derivation in of Eqs. 1-3):

Eq. 1 $$h = \beta_1 d^{2/3}\left(1 - \beta_2 d^{1/3}\right)^{2/3}.$$

Moreover, based on MET assumptions (area-preservation implies that the aggregated total tree volume is modelled as a cylinder, see Fig. 2) we also deducted that tree agb as a function of both its d and h ($agb \sim f(d,h)$) must necessarily be:

Eq. 2 $$agb = \beta_3 \rho d^2 h,$$

where ρ is averaged wood density of the tree. It is worth noting that Eq. 2 implies that biomass is directly proportional to volume (i.e. an exponent equal to 1). Consequentially, the gMET h-d model form (Eq. 1) can be propagated into Eq. 2, giving a gMET agb-d model:

Eq. 3 $$agb = \beta_1 \beta_3 \rho d^{8/3} \left(1 - \beta_2 d^{1/3}\right)^{2/3},$$

where $\beta_{1\text{-}3}$ represent coefficients that can be mechanistically deducted through tree parameters established by MET and associated scalars (see Eqs. 8, 11 and 20 in Methods). The values of β_1 and β_2 are equivalent in Eq. 1 and Eq. 3, and are constituted by a series of tree parameters which are all measurable and could be determined at a species-specific or any other relevant taxonomic level. In turn, β_3 we can be approximated to $\beta_3 \approx c \cdot \pi/6$ (where c is a unit conversion factor, see Eq. 20) under MET assumptions (area-preservation models the aggregated total tree volume as a cylinder, whereas the optimum vessel taper models the aggregated volume of conductive material as a cone, see Fig. 2).

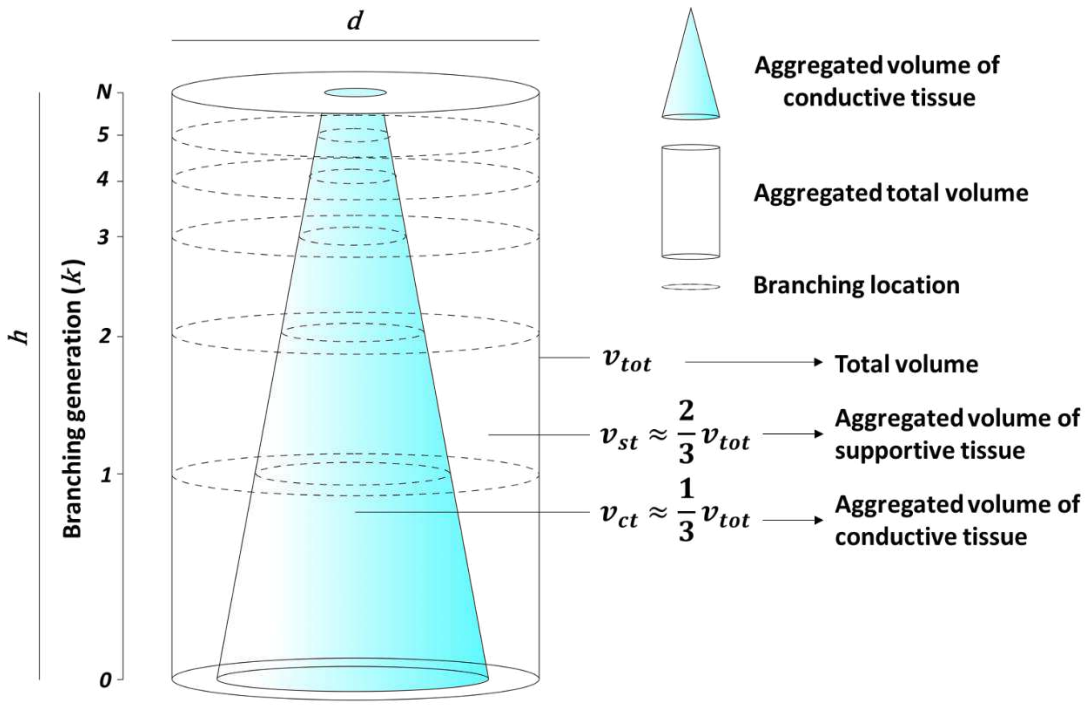

130

131 **Fig. 2 | Truncated Cone & Cylinder approximation of tree volumes.** This visualization

132 illustrates the modelization of aggregated volumes of conductive tissues across branching

133 generations (blue cone) within the total volume (cylinder).

134

The consequence of $\beta_{1\text{-}3}$ being entirely set out by MET[2] (see Eqs. 8, 11 and 20) is that the allometric models are completely mechanistic, and thus can circumvent the need for statistical fitting procedures. The revised models retain many of the inferences of the original MET, given that their derivation is directly built upon the pre-existing theory. Note that the value $\beta_2 \sim 0$ can be asymptotically approached, which yields the original scaling relationships of 2/3 for h (Eq. 1) and 8/3 for agb (Eq. 3). Thus, Eqs. 1 and 3 are more generalized expressions of the MET scaling relationships, which become relevant only in tree species with traits that make β_2 of relevant magnitude (e.g. small petioles and/or large proportion of vessels within them). This explains the apparent lack of empirical fit observed for the original MET scaling in some cases only[11,17-19,36]. The resulting implication of the gMET modifier in Eqs. 1 and 3 compared with the original MET scaling is that it reduces the rate of increase in h and agb as the tree grows in d, thus being more relevant in larger trees.

Results

Since our generalized MET models are mechanistically derived, in principle they should be able to carry out a prediction for individual trees, provided actual measurements for the tree parameters in Eqs. 8, 11 and 20. While there is no such type of data available to prove the global validity of our models, we can still use available global datasets to obtain statistically-fitted values of $\hat{\beta}_{1\text{-}3}$ (see model fitting procedures in Methods), compare their reliability against their original models[19,27], and evaluate the mechanistic significance of the resulting values in terms of the plausibility of ensuing values for the tree parameters in Eqs. 8, 11 and 20 (see Monte Carlo simulations in Methods). Thus, to test our gMET

158 models, we carried out statistical fits against worldwide data compiled for pantropical[27]
159 and global allometry[19]. Estimated values for coefficients $\hat{\beta}_{1\text{-}3}$ in Eqs. 1-3 were therefore
160 fitted using these datasets, with stratifications based on tree functional type and biome
161 across the global dataset (*sensu* Jucker *et al.*[19]). Furthermore, to give a fair comparison
162 between the gMET models and the models created by Chave *et al.*[27], the environmental
163 stress parameter (E) generated by Chave *et al.*[27] was integrated into a subset of our gMET
164 models (see model fitting procedures in Methods). The E parameter combines factors that
165 explain hydraulic constrains to tree growth, namely the temperature and precipitation
166 seasonality and climatic water deficit.
167
168 **Height-diameter model.** Table 1 shows the results of the h-d models fit through maximum
169 likelihood estimation (MLE) (see model fitting procedures in Methods), including
170 estimates and standard errors for $\hat{\beta}_1$ and $\hat{\beta}_2$, as well as their respective coefficients of
171 determination (R^2) root mean squared differences (RMSD) and mean differences (MD).
172 The 2/3 scaling relationship originally predicted by MET showed a clear lack of fit to the
173 data, with a bias most prevalent for larger trees, especially for angiosperms in tropical,
174 temperate mixed forest, woodland and savanna (Table 1 plus Supplementary Table 1, and
175 Fig. 3 plus Supplementary Fig. 1). For this reason, the prevalent pantropical allometric
176 model derived by Chave *et al.*[27] diverges significantly from the 2/3 scaling rule.
177

178 **Table 1 | Summary of adjusted tree height h-d models.**

Model	No. Observations	Coefficient Estimates $\widehat{\beta}_1$ (SE)	$\widehat{\beta}_2$ (SE)	Model Evaluation R^2	RMSD (%)	MD (%)
Chave *et al.*[27] data						
2/3 Scaling	4,004	44.2 (0.035)	-	0.73	5.59 (34.9)	-0.308 (-1.923)
Chave *et al.* model[27] (with E)	4,004	-	-	0.87	3.82 (23.8)	-0.393 (-2.448)
gMET (with E)	4,004	66.7 (0.857)	0.530 (0.002)	0.88	3.80 (23.7)	-0.065 (-0.406)
gMET (without E)	4,004	52.0 (0.105)	0.276 (0.004)	0.74	5.52 (34.4)	0.108 (0.674)
Jucker *et al.* [19] data						
2/3 Scaling	79,335	46.5 (0.037)	-	0.70	5.00 (31.5)	-0.325 (-2.042)
Whole dataset	79,335	59.6 (0.148)	0.433 (0.004)	0.72	4.86 (30.5)	0.157 (0.991)
Gymnosperms	18,958	50.9 (0.222)	0.182 (0.006)	0.75	4.32 (25.6)	0.154 (0.916)
Boreal	4,942	45.2 (0.230)	0.006 (0.015)	0.63	2.97 (22.4)	0.026 (0.196)
Temperate Coniferous	9,539	48.7 (0.123)	0.038 (0.006)	0.83	4.06 (22.6)	0.130 (0.721)
Temperate Mixed	3,419	69.4 (0.146)	0.587 (0.003)	0.63	5.03 (24.8)	0.218 (1.073)
W&S	1,058	40.4 (0.100)	0.419 (0.004)	0.59	3.29 (26.2)	0.071 (0.567)
Angiosperm	60,376	61.5 (0.147)	0.474 (0.004)	0.71	5.00 (32.1)	0.156 (1.000)
Boreal	546	74.9 (0.042)	0.494 (0.001)	0.79	1.91 (10.8)	0.031 (0.175)
Temperate Coniferous	3,366	62.8 (0.110)	0.386 (0.003)	0.76	4.01 (25.1)	0.072 (0.455)
Tropical	32,251	65.1 (0.112)	0.482 (0.003)	0.77	4.84 (29.4)	0.118 (0.717)
W&S	10,591	38.5 (0.192)	0.217 (0.013)	0.50	4.33 (49.8)	0.124 (1.426)
Temperate Mixed						
Australasia	2,493	56.8 (0.069)	0.621 (0.001)	0.77	4.29 (26.8)	0.091 (0.564)
Paleartic	8,007	89.1 (0.098)	0.701 (0.001)	0.67	3.33 (18.2)	0.033 (0.178)
Neoartic	3,122	74.7 (0.090)	0.740 (0.001)	0.79	3.69 (17.2)	0.149 (0.692)

179 gMET: generalized metabolic ecology theory model (Eq. 1). E: environmental stress parameter[27]. W&S: woodland and savannas. SE:
180 standard error of coefficient estimate. R^2: coefficient of determination. RMSD: root mean squared differences (in meters, and percentage
181 of observed mean). MD: mean differences (in meters, and percentage of observed mean).

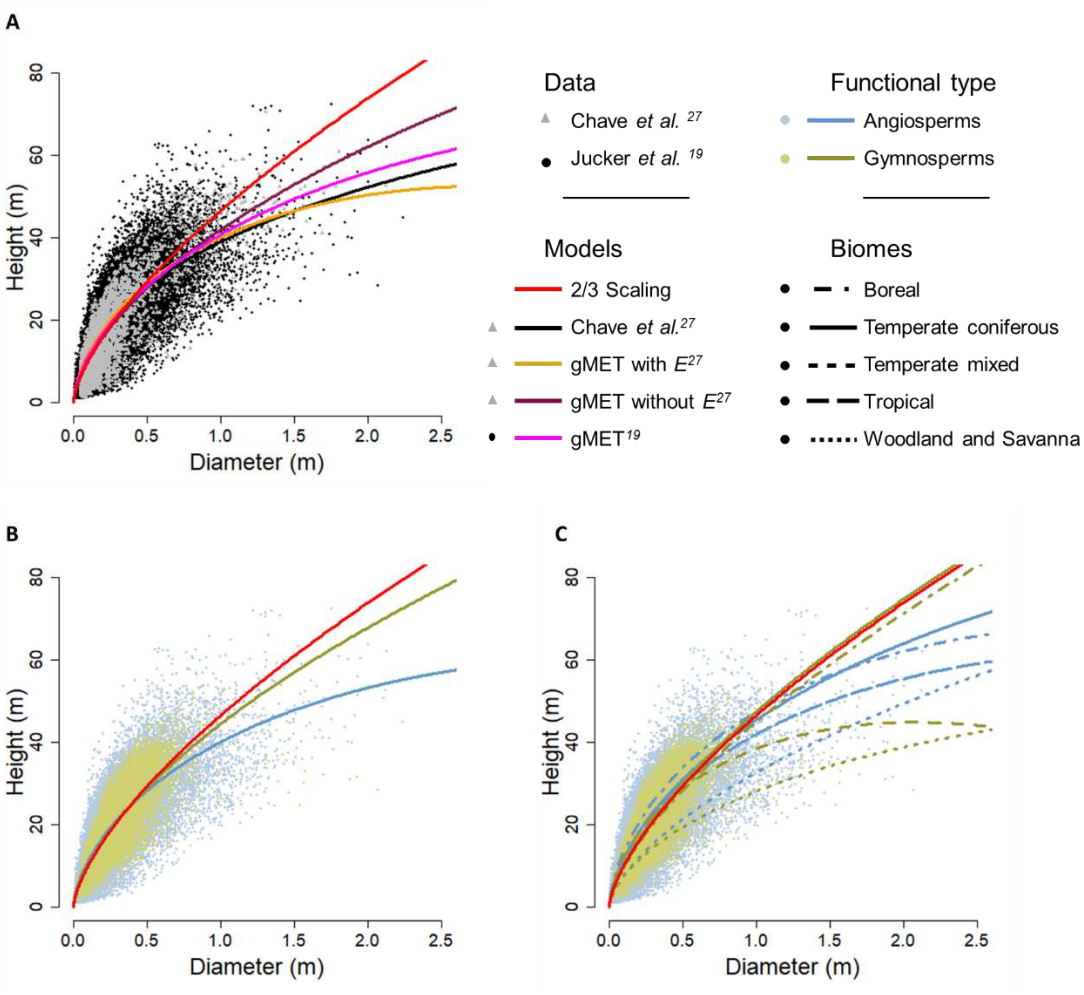

182

183 **Fig. 3 | Height-diameter model results.** Comparisons of height-diameter h-d models
184 against the 2/3 scaling rule (in red). (**A**) Our generalized metabolic ecology theory (gMET)
185 model for h (Eq. 1) adjusted to empirical data from either Chave *et al.*[27] (grey triangles) or
186 Jucker *et al.*[19] (black dots), also comparing against Chave *et al.*'s h-d quadratic log-log
187 model[27]. (**B**) gMET h-d models adjusted by functional group (*sensu* Jucker *et al.*[19]):
188 gymnosperms versus angiosperms. (**C**) gMET h-d models adjusted by functional group /
189 biome combination[19]. E: environmental stress parameter[27].

190

Our h-d gMET model outperformed both the 2/3 scaling rule and the pantropical model of Chave *et al.*[27] (Table 1). These gave slightly biased mean predictions of tree heights (MD = -0.309 m and -0.393 m), which were improved to just -0.065 m by the gMET model. Additionally, the RMSD of 3.80 m obtained by gMET was also an improvement compared to the 2/3 scaling and even to the 3.82 m RMSD obtained by the model fitted by Chave *et al.*[27] with that same data. This implies that the model form proposed in Eq. 1 is most appropriate, and betters both the simpler 2/3 scaling relationship and the quadratic log-log model form chosen by Chave *et al.*[27].

The deviation from the 2/3 scaling law was more notable in angiosperms than in gymnosperms (Fig. 3B). This effect could be recognized through the marked difference in their estimates for $\hat{\beta}_2$ (Table 1). When considering functional type and biome combinations (Fig. 3C), both the boreal and temperate coniferous gymnosperm models generated statistically non-significant values for $\hat{\beta}_2$. In those cases, $\hat{\beta}_2$ was negligible (0.006 and 0.038) and statistically non-significant (Supplementary Table 1), virtually eliminating the effect of the gMET modification (Supplementary Table 2). On the other hand, the angiosperms within the temperate mixed biome were too heterogeneous to fit a single valid model across the entire stratum (i.e. results using the entire stratum were non-significant). For this reason, this biome was split into its biogeographic zones – Nearctic, Palearctic, and Australasia –, which yielded better biogeographic zone-specific models (Table 1 and Supplementary Fig. 1).

Both β_1 and β_2 can be considered as a function of tree parameters, given Eqs. 8, 11 and 20. To investigate the plausibility of the statistically fitted values obtained in Table 1, we carried out Monte Carlo simulations using realistic values of the tree parameters

involved at each of them, to generate biologically plausible joint distributions of β_1 and β_2. The results (Figs. 4A-B) demonstrate that the values $\hat{\beta}_1$ and $\hat{\beta}_2$ obtained empirically (Table 1) are biologically plausible, as they conform with realistic values of tree parameters in Eqs. 8 and 11. Moreover, Figs. 4C-D give the model trajectories generated from 95% confidence intervals of the Monte Carlo simulations, showing that the majority of the field observations are contained within these intervals.

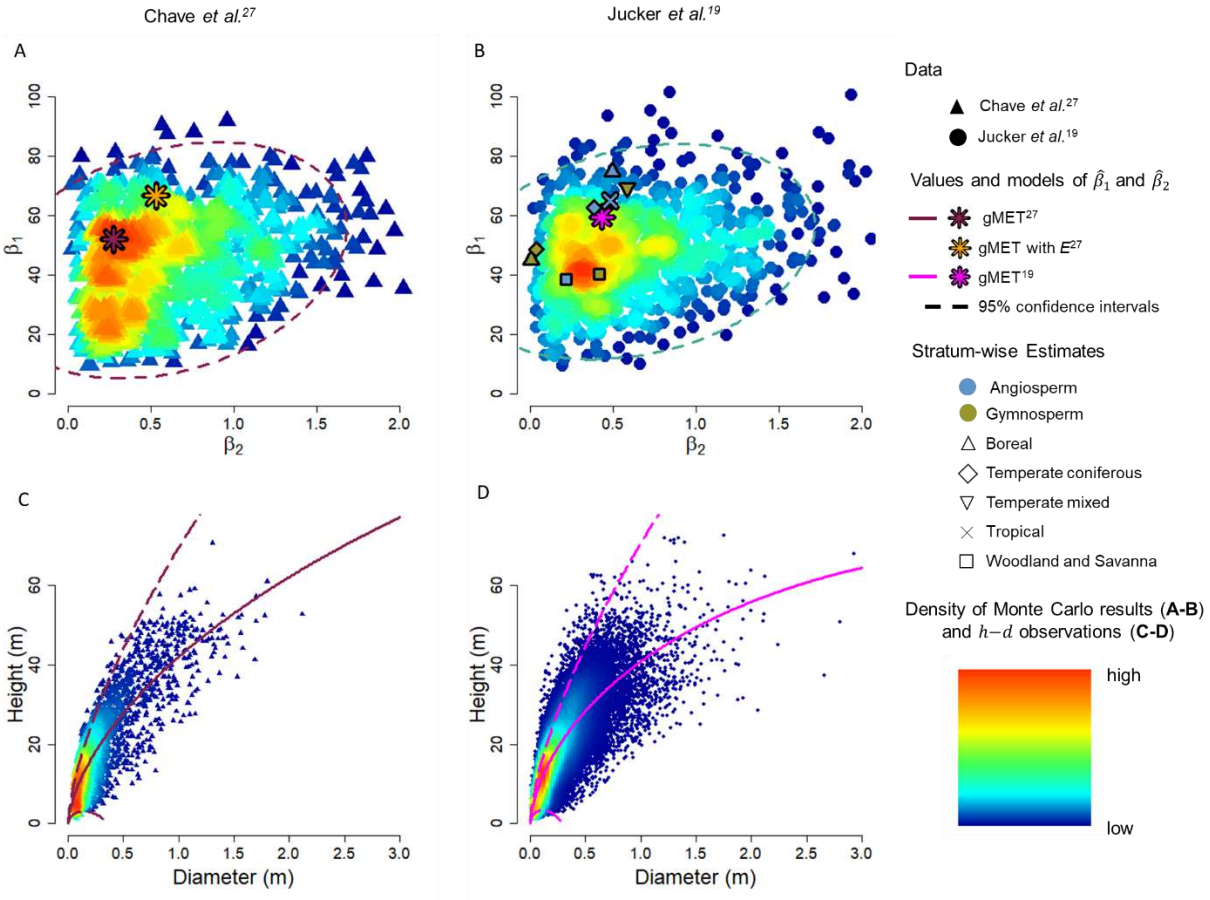

Fig. 4 | Monte Carlo results, and their confidence intervals propagated on height diameter models. Monte Carlo simulations compared against estimated $\hat{\beta}_1$ and $\hat{\beta}_2$ values. (**A-B**) Density plots of β_1-β_2 join distributions generated through Monte Carlo simulations, for both pantropical[27] (A) and global[19] (B) datasets, with 95% confidence intervals given obtained through a χ^2 distribution. (**C-D**) Monte Carlo simulation-derived 95% confidence interval values for β_1 and β_2, propagated into the h-d gMET (without E) model.

Biomass-Diameter model. The agb-d models (Eqs. 2-3) were tested only against Chave *et al.*[29] data, because it was the only dataset that incorporated all the predictors needed (ρ, d and h). Prior to reflecting on the $agb \sim f(d)$ relationship, it is noteworthy to consider the relationships using both tree height and diameter as predictors to above ground biomass ($agb \sim f(d,h)$). Chave *et al.*'s[27] widely used pantropical model $agb = 0.0673 \cdot (\rho d^2 h)^{0.976}$ (n.b. diameter given in cm) was compared against the equivalent gMET derived equation, with the form $agb = \beta_3(\rho d^2 h)$ (Eq. 2). The derivation of β_3 under MET assumptions (Eq. 20) is equivalent to $\beta_3 = 524$ (or $\beta_3 = 0.0524$ if diameter is given in cm). With no fitting procedure involved, the $agb \sim f(d,h)$ theoretical equation derived from MET (Eqs. 2 and 20) yielded an R^2 of 0.911, an RMSD of 1.17 Mg and a MD of 0.034 Mg, values that barely differed from an MLE estimation of $\hat{\beta}_3 = 527$ which increased the bias (Table 2). The theoretical gMET models achieved a better R^2 and RMSD than the statistical fit of Chave *et al.*'s[27], although they were slightly more biased. These $agb \sim f(d,h)$ models are limited by the requirement of h measurements, which are often unavailable[29,30] and thus the validity of the gMET $agb \sim f(d)$ relationship was considered further.

Table 2 | Summary of adjusted tree biomass agb-d models.

Model	$\widehat{\beta}_3$ (SE)	R^2	RMSD (%)	MD (%)
$agb \sim f(d, h)$				
Chave *et al.*[27] model (without E)	-	0.905	1.207(106.4)	-0.002(-0.204)
Theoretical MET $\beta_3 = c \cdot \pi/6$	-	0.911	1.166(102.8)	0.034 (2.997)
Theoretical MET	527.0 (1.882)	0.911	1.166(102.8)	0.041 (3.587)
$agb \sim f(d)$				
8/3 Scaling	472.8 (2.249)	0.890	1.300(114.6)	-0.030(-2.640)
Chave *et al.*[27] model (with E)	-	0.871	1.404(123.8)	-0.003(-0.272)
gMET $\beta_3 = c \cdot \pi/6$ (with E)	-	0.873	1.394(122.9)	0.029(2.550)
gMET $\beta_3 = c \cdot \pi/6$ (without E)	-	0.888	1.309(115.5)	0.044(3.909)
gMET (with E)	526.6 (2.396)	0.881	1.350(119.0)	0.032(2.815)
gMET (without E)	507.7 (2.430)	0.889	1.304(114.9)	0.008(0.682)

Theoretical MET: $agb \sim f(d, h)$ model (Eq. 2). gMET: generalized metabolic ecology theory $agb \sim f(d)$ model (Eq. 3). SE: standard errors of coefficient estimates. R^2: coefficient of determination. RMSD: root mean squared differences (in Mg, and percentage of observed mean). MD: mean differences (in Mg, and percentage of observed mean). gMET models under $agb \sim f(d, h)$ use predicted heights from their respective h-d models, while gMET $agb \sim f(d)$ models adhere explicitly to Eq. 3. $\beta_3 = c \cdot \pi/6$ signifies that the theory-based value (Eq. 20) has been used, with no MLE procedure involved. All these were tested with the 4,004 observations of Chave *et al.*'s[27] pantropical dataset.

The gMET allometry for $agb{\sim}f(d)$ (Eq. 3) was employed by propagating values of $\hat{\beta}_1$ and $\hat{\beta}_2$ from each associated $h{\sim}f(d)$ model (Table 1), and subsequently either fitting β_3, or assuming the value of $\beta_3 = c \cdot \pi/6$ in Eq. 20 (i.e. involving no fitting procedures). All alternatives outperformed Chave et al.'s[27] $agb{\sim}f(d)$ model (Table 2 and Fig. 5A). Generally, the gMET models excluding E performed best. 95% confidence intervals for this model (Figs. 5B and 5D) were generated by propagating the Monte Carlo simulation results for β_1 and β_2 (Figs. 4A-B) to the $agb{\sim}f(d)$ equation, again demonstrating that the realistic variation in β_1 and β_2 adequately encompasses the majority of field observations. The best performing $agb{\sim}f(d)$ model (in terms of R^2 and RMSD) proved to be that of the original 8/3 scaling, although it was more biased (MD = -0.030) than Chave *et al.*'s[27] and the best gMET model. The comparison of the $agb{\sim}f(d)$ models is shown in Fig. 5A illustrates that the model trajectories have only slight differences. Thus, generally speaking the choice of agb-d model matters less than for h-d, although one must consider the uncertainty in terms of relative error implied by the use of these models (RMSD = 10.8-49.8 % for h, and RMSD = 102.8-123.8 % for agb).

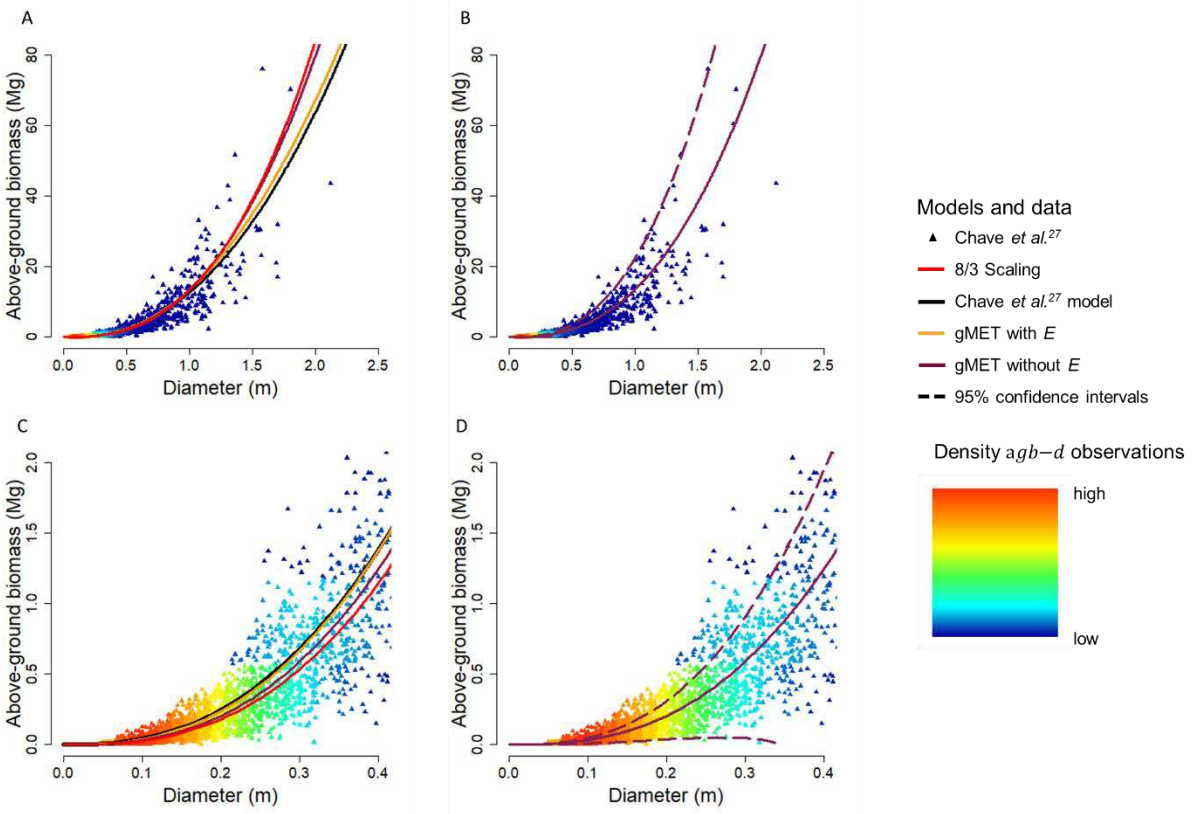

Fig. 5 | Above-ground biomass-diameter model results. Comparisons of biomass-diameter agb-d models against the 8/3 scaling rule (in red). (**A**) Our generalized metabolic ecology theory (gMET) model for agb (Eq. 3) adjusted to empirical data from Chave *et al.*[27] is presented (with and without E), compared against Chave *et al.*'s[27] agb-d quadratic log-log model. E: environmental stress parameter[27]. (**B**) Monte Carlo simulation-derived 95% confidence interval values for β_1 and β_2 (Fig. 2C), propagated into the agb-d gMET (without E) model. (**C-D**) enhancements of panels A and B showing only the data for smaller trees.

Discussion

Our results demonstrate that the gMET relationships are unbiased and show a significant level of empirical fit to global tree datasets that make them universally applicable. We also show that the statistical fit to data yields coefficient values that are plausible for realistic magnitudes of the tree parameters involved in Eqs. 8, 11 and 20, demonstrating the biological relevance of our gMET advances from the original MET. The main asset of the gMET models is their mechanistic derivation underpinned by MET assumptions. Remarkably, the theory based gMET models outperformed the statistical models of Chave *et al.*[27] using their complied dataset. These results support MET itself, resolving the criticism pertaining to the lack of empirical support to MET scaling for large trees and tropical areas[11,17-19,36]. Furthermore, gMET concurrently allows for the original MET scaling law ($\beta_2 \sim 0$), explaining why the original MET scaling relationships fit adequately in some scenarios.

The gMET h-d model proposed (Eq. 1) performed exceptionally well, demonstrating a marked improvement upon both the original 2/3 scaling law and the widely used pantropical model by Chave *et al.*'s[27] (Table 1 and Fig.3). It was superior to the 2/3 scaling against global data[19], especially for angiosperms, and also gymnosperms at lower latitude biomes (Tables 1 and Supplementary Tables 1-2). Moreover, the simple $agb \sim f(d, h)$ model based on MET assumptions (Eq. 2) outperformed Chave *et al.*'s[27] pantropical model (Table 2). The propagation of the gMET $h \sim f(d)$ model to derive Eq. 3 ($agb \sim f(d)$) gave results comparable to the original 8/3 scaling law and Chave *et al.*'s[27] model (Table 2 and Fig. 5). Nonetheless it should be noted that at the agb-d level our study could only test against the pantropical dataset. Global data including agb measured through destructive sampling is needed to still clarify functional type and biome dependencies for the agb-d relationship. We also recommend that further research focuses on acquiring empirical measurements of the tree parameters involved in Eqs. 8 and 11, because once sufficient data becomes available the gMET models could

potentially become grounds for determining tree biomass in the field and circumvent the need for destructive sampling.

A clear difference between tree functional types was evident within the $\hat{\beta}_2$ results (Table 1 and Figs. 3B-C), likely due to divergences at the cellular level. Disparities in the tree parameters influencing β_2 (Eq. 11) have indeed been observed between angiosperms and gymnosperms[34,39]. Angiosperms have differentiated cell types, vessels and fibres, each dedicated to conductive and supportive functions respectively. This tissular differentiation brings about a functional separation at different areas within the cross-section of the tree stem, which other authors have referred to as lumen and non-lumen fractions (for CT and ST respectively)[37,38]. Alternatively, gymnosperms have integrated conductive and supportive functionality in their tissues through tracheids, and this functional integration of tissue leads to greater deviations from Murray's law for gymnosperms than angiosperms[43]. Thus, the limitation in the h of a tree is more regulated by mechanical constraints in gymnosperms (MET), while angiosperms tend towards hydraulic constraints (Eq. 10 in Methods), with gMET effectively integrating both controls.

There were notable levels of variation in the estimated $\hat{\beta}_1$ and $\hat{\beta}_2$ values across biomes, which gives clues on their biological relevance. All values were included within the distributions of plausible coefficient values, which we derived from reasonable values of tree parameters (Eqs. 8 and 11) via Monte Carlo simulations (Fig. 4). Environmental factors are likely to explain the variance across biomes in species of the same functional type, with β_1 and β_2 changing in accordance to plant survival strategies, given that tree parameters (such as vessel dimensions) change according to the environment[46]. Stratum-wise estimations of $\hat{\beta}_{1-2}$ therefore reflect the combinations of optimal tree parameters for the growth and survival of a given species in its typical habitat. This idea is also reinforced by the high proportion of explained variability added by E in the gMET h-d model. It should be pointed out that our use

of E within the gMET models (Eqs. 23 and 26 in Methods) is contentious, given the calculation of E is intrinsically linked to models created by Chave *et al.*[27]. Further research should be devoted to find the mechanistic integration of the factors intrinsically included in E – temperature and precipitation seasonality, and water deficit – in the gMET model: how they affect the tree parameters involved in β_1 and β_2 (Eqs. 8 and 11)[47], given that specific species traits could compensate for the hydraulic constraints on tree growth that these factors impose.

Regarding the agb-d relationship, it is important to point out that while many authors such as Chave *et al.*[27] adjust coefficients using models of the form $agb = \beta_3(\rho d^2 h)^{\beta_4}$, our derivation from MET assumptions (area preservation) implies that the exponent must necessarily be $\beta_4 = 1$ (Eq. 2). We also provided grounds for the mechanistic determination of β_3 from the proportion of volume of supportive material (v_{st}). While the $\hat{\beta}_3$ estimations in Table 2 were around the $\beta_3 \approx c \cdot \pi/6$ value approximated through MET, there are two obvious challenges to the assumptions employed. Firstly, it was assumed that the density of supportive tissue (ρ_{st}) is approximate to the measured wood density $\rho \sim \rho_{st}$. This brings a bias because ρ can only be systematically lower than the actual ρ_{st}. The second assumption relates to the modelization of the aggregate volume of conductive material, as a complete cone within a stem represented as a cylinder (Fig. 2), with $CT_0 = 1$ at the base of the tree and $CT_N = 0$ at tip of the petiole, meaning v_{st} equates to 2/3s of the cylinder's volume (Eq. 18 in Methods). In reality CT cannot reach either of these values at the extremes, so the cone is in fact truncated (Fig. 2). This brings another bias because the actual factor of v_{st} over the total volume must be necessarily higher than 0.66. We cannot quantify this bias in practice. However, these two systematic deviations from our assumptions counteract each other (the more volume of supportive material, the closer wood density approximates the density of supportive material), cancelling out and effectively minimising the divergence from the assumed $\beta_3 \approx 524$. Since ρ is typically 10-15% lower than ρ_{st}[37], the actual proportion of supportive material within the

357 total volume must approximately be 0.73-0.76. Thus, the empirical disparities from the value
358 proposed in Eq. 20 are in fact small divergences from a perfect trade-off between these two
359 breaches of the underlaying assumptions.
360
361 **Conclusions and future perspectives**

362 We present new generalised equations that make a crucial advance for MET through
363 the consideration of differentiated tissue functions. These equations are characterised by
364 theory-determinable exponents and coefficients, allowing for a fully generalised and globally
365 applicable model form. The exponents are fixed by MET scaling, whereas the coefficients are
366 defined by tree traits that vary with biome and tree functional type, likely driven as adaptations
367 to different bioclimatic conditions. We showed that our models outperform statistically fitted
368 models that are widely used for large scale agb and forest carbon estimation[27]. Our gMET
369 models should provide a new avenue of scientific development towards global theory-based
370 models for tree allometry, giving a possibility to mechanistically link histological and
371 macroscopic traits. They will also pave the way for large scale, accurate agb and forest carbon
372 estimation globally, utilising new methods and technology such as satellite lidar available
373 through the Global Ecosystem Dynamics Investigation (GEDI) mission.
374

Methods

Theoretical basis for generalized Metabolic Ecology Theory (gMET) models and notation. Metabolic Ecology Theory (MET) models trees as a continually branching hierarchical networks, running from the trunk to the petiole. The volume filling network produces a self-similar fractal[1,2] leading to relationships for the diameter (d_k; m) and length (l_k; m) of a parent branch (k) scaling from those of its daughter branch ($k+1$) (Fig. 1):

Eq. 4 $$\frac{d_{k+1}}{d_k} = n^{-1/2};$$

Eq. 5 $$\frac{l_{k+1}}{l_k} = n^{-1/3},$$

where n denotes the number of daughter branches that a parent branch splits into (typically $n = 2$), and $k = 0,1,\dots,N$ are the branching generations from the trunk ($k = 0$) to the petiole ($k = N$). MET postulates that area is preserved across all branching generations (Eq. 4), and that the system is a volume-filling network (Eq. 5). As the network is continuously branching, its total length ($l_t = \sum_{k=0}^{N} l_k$) can be deduced through an infinitely scaling geometric series[2]:

Eq. 6 $$l_t = \frac{l_0}{(1-n^{-1/3})},$$

where l_0 denotes the length of the trunk, and l_t is equivalent to the total height (h; m) of the tree[33]. In our notation the diameter measured at the breast height (d; m) is also equivalent to d_0. Using these formulae, the h-d allometric equation can be derived as[2]:

Eq. 7 $$h = \beta_1 d^{2/3},$$

where β_1 denotes a scalar:

Eq. 8 $$\beta_1 = \frac{l_N}{(1-n^{-1/3}){d_N}^{1/3}},$$

which becomes species-specific because it is regulated by tree parameters that can be determined at species-level: the length (l_N), and diameter (d_N) of the last branching generation (N), and the number n of daughter branches a species makes from each parent branch.

West *et al.*[2] concluded that the $h \propto d^{2/3}$ scaling relationship derives from an area preserving and volume filling network as shown in Eqs. 4-5. They noted, along with previous literature[40,41], that the $2/3$ scaling exponent is the optimal relationship between l_k and d_k in order to resist buckling (mechanical constraint). By extension, the scaling exponent should be considered to apply to the area that gives mechanical structure. On the other hand, conductive area that does not generate mechanical strength should not necessarily scale to $2/3$, and must be regulated by hydraulic limitations instead[33]. Moreover, key to MET is that an individual's size scales with its resource distribution network[1]. West *et al.*[2] outlined how an optimum taper of conducting tissue within the branching network leads to a scaling relationship between the proportion of conductive tissue at each generation (CT_k) and d_k, such that $CT_k \propto {d_k}^{1/3}$. This tapering minimises energy expenditure for resource movement creating a hydraulic limitation to the potential maximum h that the tree could reach (hydraulic constraint). We postulate that this same limiting factor affects the mechanical limitations as well, because the proportion of conductive tissue within a cross-section of the trunk (CT_0, which will hereby be referred to as CT) also increases as the tree grows in size, scaling[2] to its d as $CT \propto d^{1/3}$. Since the mechanical limitation only applies to the supportive tissue and the conductive tissue plays no part in supporting the branching network[42,43], we propose that $h \propto d^{2/3}$ scaling applies only to the proportion of tissue that has supportive function (ST) (Fig. 1). This proposition effectively combines both the mechanical and hydraulic limitations into one, and it is the basis for the development of our generalized MET-based (gMET) allometry.

Theory development for the generalized MET *h-d* allometric relationships. Alternatively to Eq. 7, we propose the true scaling relationship should give h as a function of only the proportion of d that supports the branching network, that is the proportion of supporting tissue, i.e. that primarily consisting of fibres, within a cross-section of the trunk (ST_0, which will hereby be referred to as ST):

Eq. 9 $$h \propto (STd)^{2/3}.$$

Moreover, MET also states that the proportion of conductive tissue CT within a given individual is proportional to $d^{1/3}$, with an exponent of $1/3$ derived from the rate of optimum vessel taper[2]:

Eq. 10 $$CT = \beta_2 d^{1/3},$$

where β_2 denotes a scalar that is determinable within MET[2] using the diameter (d_N) of the final branching generation, the number of conductive vessels within that petiole (n_N) and the radii of each of these vessels (a_N; m):):

Eq. 11 $$\beta_2 = \frac{4a_N^2 n_N}{d_N^{7/3}} = \frac{4a_N^2 n_N}{d_N^2 d_N^{1/3}} = CT_N d_N^{-1/3},$$

or alternatively through CT_N which is the proportion of conductive material within a cross-section of the final branching generation (petiole). Eq. 11 shows that β_2 can be modelled as the ratio between CT_N and ${d_N}^{1/3}$, although the interpretation of the parameter is better considered through Eq. 10 which shows that the ratios between the dimensions of trunk and petiole, d to d_N, and their respective proportions of conductive (lumen) material, CT to CT_N, are consistent with the hydraulic constraint. Following Eq. 10, as $ST = 1 - CT$ (Fig. 1), the proportion of supportive material can be given as:

Eq. 12 $$ST = 1 - \beta_2 d^{1/3}.$$

441 ST incorporates all types of tissue that can have supporting function within the trunk,
442 comprising of any non-conductive tissue (non-lumen) which includes fibres[37,38]. Applying Eq.
443 12 as a modifier to the scaling law therefore allows the interconnection between tissue types to
444 be addressed within the model only using d, whereby only structurally relevant tissue is scaled
445 to $2/3$:

446 Eq. 13 $$h = \beta_1 \left(d\left(1 - \beta_2 d^{1/3}\right)\right)^{2/3} = \beta_1 d^{2/3}\left(1 - \beta_2 d^{1/3}\right)^{2/3}$$

447 This gMET h-d allometric model (Eq. 1) based on a combination of MET scaling
448 relationships includes the interconnection between the two tissue functional types: hydraulic
449 constraints regulated by the tapering of conductive tissue and mechanical stability regulated by
450 the proportion of supportive tissue, both bringing about a combined limitation to h. The
451 mechanical constraint is predominant in large trees as they need an increasing CT, compared
452 with smaller plants, to overcome hydraulic constrains to the upward flow of sap, and for that
453 reason the CT scales itself to d as they grow (Eq. 10). Consequently, the effect of this
454 component (Eq. 12) in the scaling relationship (Eq. 9) becomes more prominent for larger trees,
455 which thus depart more from the original MET h-d $2/3$ scaling law. On the other hand, Eq.
456 11 shows that the value of β_2 depends on a_N, n_N and d_N, none of which can be physically null
457 in a living individual and thus β_2 must necessarily be a non-zero positive value ($\beta_2 \neq 0$).
458 However, certain combinations of these tree parameters can overall make the proportion of
459 conductive tissue in the petiole CT_N small, making $\beta_2 \sim 0$ negligible in practice (see Monte
460 Carlo simulations in Methods), and thus the original MET h-d $2/3$ scaling law approaches
461 such cases well. Therefore, our allometric model in Eq. 13 is a generalized version of the
462 original MET $2/3$ scaling, rather than a substitution of it.

463

Theory development for the generalized MET agb-d allometric relationships. Based on the same MET assumptions and constraints, West *et al.*[2] also derived a $8/3$ scaling law between the diameter of a tree and its biomass, and we can similarly propagate our gMET relationships to yield tree biomass. The aboveground biomass (agb; kg) of a tree is calculated by multiplication of the aboveground volume of its supportive (lumen) material (v_{st}; m^3) times the average density of lumen material (ρ_{st}; $g \cdot cm^{-3}$):

Eq. 14 $$agb = c\rho_{st}v_{st},$$

where c is a unit conversion factor. The volume of supportive material can be derived by subtracting the volume of its conductive (non-lumen) material (v_{ct}) from the total volume (v_{tot}):

Eq. 15 $$v_{st} = v_{tot} - v_{ct}.$$

Under the assumption of area preservation (Eq. 4), v_{tot} can be modelled as a cylinder (as aggregated volume of the entire branching network $k = 0$-N (i.e. not just the tree trunk; Fig. 2):

Eq. 16 $$v_{tot} = \frac{\pi}{4}d^2h.$$

Under the hydraulic constraint (Eq. 10), the aggregated volume of conductive material for the entire branching network can be modelled as a cone (Fig. 2), and thus:

Eq. 17 $$v_{ct} \approx \frac{1}{3}\frac{\pi}{4}d^2h.$$

These lead us to a value for v_{st} approximated under these assumptions:

Eq. 18 $$v_{st} \approx \frac{2}{3}\frac{\pi}{4}d^2h.$$

Fig. 2 illustrates that this cone must be truncated at both its base and tip, since neither $CT_0 = 1$ nor $CT_N = 0$ would be plausible within a natural system. However, empirical results showed

that the value $v_{st} \approx \frac{2}{3} v_{tot}$ works well as an approximative assumption (see discussion in the main article).

Furthermore, ρ_{ST} is rarely collected due to the complex and time-consuming methods required for its measurement[8], despite it being a relevant tree parameter[37,38,46]. Instead, the tree averaged wood density (ρ) is typically obtained as dry weight over fresh volume of biomass, and a factor can be used to derive one from another[38]. Nonetheless, their values are very similar in practice[37], and thus here we can proceed under the assumption that $\rho_{st} \sim \rho$, and substitute Eq. 18 in Eq. 14 (see discussion):

Eq. 19 $$agb = \beta_3 \rho d^2 h,$$

which is a theoretical MET-based $agb \sim f(d,h)$ allometric model (Eq. 2). β_3 denotes a scalar which under the above-mentioned assumptions (Eq. 18) must approximate:

Eq. 20 $$\beta_3 \approx c \frac{2}{3} \frac{\pi}{4}.$$

The unit conversion factor equals $c = 10^3$ for the customarily used units stated above, which yields a value of $\beta_3 = 10^3 \cdot \pi/6 = 524$. If centimetres are employed for d the overall factor becomes $c = 10^{-1}$ which yields $\beta_3 = 0.0524$, which is more comparable to allometric coefficients estimated by other authors such as Chave *et al.*[27].

While Eq. 19 provides a model to predict the agb of a tree from its measured d and h ($agb \sim f(d,h)$) it is more typical to use a model dependent upon d only ($agb \sim f(d)$). West *et al.*[2] deducted the MET agb-d $8/3$ scaling law by propagation of the h-d $2/3$ scaling law. Similarly, the theoretical development of gMET can be propagated from h-d to yield the agb-d relationship by substituting Eq. 13 in Eq. 19, yielding:

Eq. 21 $$agb = \beta_3 \rho d^2 \left(\beta_1 d^{2/3} \left(1 - \beta_2 d^{1/3}\right)^{2/3} \right) = \beta_1 \beta_3 \rho d^{8/3} \left(1 - \beta_2 d^{1/3}\right)^{2/3},$$

which is a gMET $agb \sim f(d)$ allometric model (Eq. 3). β_1 and β_2 can be directly propagated from the h-d equation, and thus retain their biophysical relevance (Eqs. 8 and 11). Thus, the inclusion of the component accounting for the scaling of supporting tissue (Eq. 9) also has a similar effect in modifying the original MET agb-d $8/3$ scaling law between tree biomass and diameter, becoming more relevant for larger trees and those with traits resulting in large values of β_2. It also concurrently allows for the original MET scaling law under $\beta_2 \sim 0$, and thus it is a generalized expression version of the original MET $2/3$ scaling, and not a substitution of it.

Model fitting procedures. To test the validity of our proposed models, we contrasted them against empirical data available from Chave *et al.*[27] and Jucker *et al.*[19], and derived the values of $\beta_{1\text{-}3}$ that could be expected from those data. It has been argued that maximum likelihood method (MLE) should be preferred for power-law estimations[48]. We decided to test both MLE and a Gauss-Newton algorithm for non-linear least squares (NLS) estimation, finding only marginal differences between them (Supplementary Table 1) and thus reporting MLE results only. Coefficients $\beta_{1\text{-}3}$ were estimated using the 'optim' function for MLE and the 'nls' function for NLS, both within the 'stats' package in the R programming environment. In the case of MLE, the standard errors were estimated via bootstrapping 100 independent draws of 500 samples each.

The h-d model (Eq. 1) was fitted with initial values $\beta_1 = 100$ and $\beta_2 = 0.2$. No issues were found in terms of local minima, with the fitting process reaching the same result for wide ranges of initial values (any values of $\beta_1 \geq 10$ and $\beta_2 \geq 0.01$ up to $\beta_2 = 0.75$ or larger depending on individual models). Our results were compared against those obtained by Chave *et al.*'s h-d model[27] using their own compiled dataset, which in their case includes an

environmental stress parameter (E) that explains a relevant portion of variance in their model (with d specified in cm):

Eq. 22 $$\ln h = 0.893 - E + 0.760 \ln d - 0.0340 (\ln d)^2.$$

Thus, to give fairer comparison against Chave *et al.*[27], we made a version of the gMET model that incorporates E in a similar manner (i.e. converted to original scale):

Eq. 23 $$h = \beta_1 e^{-E} d^{2/3} \left(1 - \beta_2 d^{1/3}\right)^{2/3}.$$

Furthermore, Jucker *et al.*'s[19] dataset contained a sample size of individual trees with measured d and h sufficient to derive separate h-d models stratified according to functional type – gymnosperms and angiosperms – and biome – boreal, temperate coniferous, temperate mixed, woodland and savannas, and tropical – combinations. In some cases, fitting these models required more refined initial guesses. The angiosperm temperate mixed biome model proved to be too heterogeneous to fit a single model valid for the entire stratum. For this reason, we split this biome into its biogeographic zones – Nearctic, Palearctic, and Australasia –, which yielded better biogeographic zone-specific models (Table 1 and Supplementary Fig. 1). An F-test for nested models was used to evaluate the significance of all these stratum-wise gMET models against the simpler 2/3 scaling (Supplementary Table 2).

The agb models (Eqs. 2-3) were tested only against Chave *et al.*[27] data, because it was the one that incorporated all the predictors needed (ρ, d and h). In this case we tested two groups of models: those predicting agb from both d and h ($agb \sim f(d,h)$), and those predicting from d only ($agb \sim f(d)$). All the agb models were developed by direct propagation the $\hat{\beta}_1$ and $\hat{\beta}_2$ from the fitted h-d results. Then we tested both our theoretical value of $\beta_3 = 524$ under MET assumptions (Eq. 20), and also estimated β_3 via MLE. For comparison, these were tested against Chave *et al.*[27] $agb \sim f(d,h)$ model using their own data (with d specified in cm):

554 Eq. 24 $agb = 0.0673 \cdot (\rho d^2 h)^{0.976}$.

555 It is noteworthy to mention that the model in Eq. 24 is equivalent to ours in Eq. 19 for $\hat{\beta}_3 =$
556 673 (due to unit conversion) and an exponent slightly diverging from 1 (i.e. not assuming area
557 preservation as in Eq. 18). Furthermore, our results were also compared against Chave *et al.*'s[27]
558 $agb \sim f(d)$ model, which again involves the use of E (with d specified in cm):

559 Eq.25 $\ln agb = -1.803 - 0.976 \cdot E + 0.976 \ln \rho + 2.673 \ln d - 0.0299 (\ln d)^2$.

560 And again, we made a version of the gMET model that incorporates E for fair comparison:

561 Eq. 26 $agb = \beta_1 \beta_3 e^{-E} \rho d^{8/3} \left(1 - \beta_2 d^{1/3}\right)^{2/3}$.

562 The initial value for the MLE estimation was $\beta_3 = 524$, again with a wide range of initial
563 values of around $\beta_3 =$ 50-3,000 reaching a same solution.

564

565 **Monte Carlo simulations.** To deduce whether the estimated values of $\hat{\beta}_1$ and $\hat{\beta}_2$ are realistic
566 in natural systems, and reflect on the biological relevance of these coefficients, Eqs. 8 and 11
567 were used within Monte Carlo simulations to obtain frequency distributions for β_1 and β_2 that
568 derive from plausible values of the tree parameters involved at each of them. These tree
569 parameters are tree architecture traits (e.g. dimensions of the stem and petiole). Some of
570 simulated values were deducted from the literature, whereas others followed logical inter-
571 dependencies among these traits. We assumed a log-uniform distribution within a range of l_N
572 values from 3 mm to 1 m[49]. The number of daughter branches that a parent branch splits into
573 was assumed to follow a geometric distribution truncated to a range $n =$ 2-6, following West
574 *et al.*[2]. Since some of the tree traits are mutually inter-dependent, as d_N invariably changes
575 with l_N and n, it would be unrealistic to draw random independent values from each of them.
576 For this reason, we modelled their relationship by rearrangement and combination of Eqs. 4-7:

577 Eq. 28 $$d_N = d_0 \left(\frac{l_N}{l_0}\right)^{3/2} = \frac{d_0 {l_N}^{3/2}}{{l_t}^{3/2}\left(1-n^{-1/3}\right)^{3/2}},$$

578 which follows from the relationship between the ratios of d_N to d_0 and l_N to l_0, i.e. the
579 dimensions of the first and last branching generations, as determined by MET assumptions
580 (Eqs. 4-5). Then, by solving l_0 in Eq. 6, it was substituted by l_t and n in the denominator,
581 generating the relationship $d_N \sim f(l_N, n, d_0, l_t)$ in Eq. 28, where l_N and n have been simulated
582 in previous steps and paired values of d_0 and l_t can be retrieved from actual empirical samples
583 (n.b. $d_0 \equiv d$ and $l_t \equiv h$). In a Monte Carlo simulation with a sample of size 1,000, we drew
584 independent samples from Chave *et al.*[27] and Jucker *et al.*[19] datasets, plus from the above-
585 mentioned assumed distributions for l_N and n, to generate a distribution of d_N values associated
586 with them. This provided a set of realistic paired values for d_N, l_N, and n which were combined
587 through Eq. 8 to derive plausible β_1 values under natural conditions.

588 Following up from the paired values obtained for β_1, a similar procedure was employed
589 to derive a distribution of plausible joint β_2 values under natural conditions. β_2 can be shown
590 as a function of d_N and CT_N. Again, the relationship of these dimensions in the petiole and the
591 trunk, d_N to d_0 and CT_N to CT_0, can be related via MET assumptions (Eq. 11):

592 Eq. 29 $$CT_N = CT_0 \left(\frac{d_N}{d_0}\right)^{1/3},$$

593 Unfortunately, datasets with CT_0 measurements along with their respective d_0 are not available.
594 To overcome this difficulty, we simulated CT_0 values assuming a non-central Beta distribution
595 $CT_0 \sim \text{NonCentralBeta}(\alpha = 2,\ \beta = 20,\ \delta = 0.1)$, which we regarded to faithfully model the
596 lumen proportions observed in the literature[37,38]. The resulting plausible distributions for β_1
597 and β_2 are shown in Figs. 2A-B, where the $\hat{\beta}_1$ and $\hat{\beta}_2$ values estimated for empirical models
598 are shown to illustrate that those values correspond well to the combination of realistic
599 assumptions in the tree parameters considered in Eqs. 8 and 11. An ellipse of 95% confidence

intervals (CIs) for β_1-β_2 combinations was derived from a χ^2 distribution with 2 degrees of freedom (Figs. 2A-B). Since any β_1-β_2 combination within that ellipse provides 95% CIs for the model, we chose to determine those that would correspond to a tallest and shortest tree with quadratic mean diameter in the dataset. In order to achieve that, we calculated the height that would correspond to quadratic mean diameter, for every β_1-β_2 combination calculated in that ellipse, and from those results we extracted values corresponding to the minimum and maximum tree height, which are those shown for the gMET h-d models in Figs. 4C-D. These were also propagated to the gMET agb-d model in Fig. 5B under the assumption of $\beta_3 = 10^3 \cdot \pi/6$ (Eq. 20). The results demonstrate that the β_1 and β_2 combinations derived from realistic values of tree parameters correspond with the empirical h-d and agb-d relationships.

References

1. G. B. West, J. H. Brown, B. J. Enquist, A general model for the origin of allometric scaling laws in biology. *Science* **276**, 122–126 (1997).

2. G. B. West, J. H. Brown, B. J. Enquist, A general model for the structure and allometry of plant vascular systems. *Nature 400*, 664–667 (1999).

3. B. J. Enquist, G. B. West, E. L. Charnov, J. H. Brown, Allometric scaling of production and life-history variation in vascular plants. *Nature* **401**, 907–911 (1999).

4. G. B. West, B. J. Enquist, J. H. Brown, Birdsong: from behavior to neuron. *Proc. Natl. Acad. Sci. U.S.A.* **106**, 7040–7045 (2009).

5. K. J. Niklas, B. J. Enquist, Invariant scaling relationships for interspecific plant biomass production rates and body size. *Proc. Natl. Acad. Sci. U.S.A.* **98**, 2922–2927 (2001).

6. E. D. Lee, C. P. Kempes, G. B. West, Growth, death, and resource competition in Sessile Organisms. *Proc. Natl. Acad. Sci. U.S.A.* **118**, e2020424118 (2021).

624 7. A. P. Allen, J. F. Gillooly, J. H. Brown, Linking the global carbon cycle to individual
625 metabolism. *Funct. Ecol.* **19**, 202–213 (2005).
626 8. C. A. Price, C. A. Price, J. F. Gilooly, A. P. Allen, J. S. Weitz, K. J. Niklas, Tansley review
627 The metabolic theory of ecology : prospects and challenges for plant biology, *New Phyl.* **188**,
628 696–710 (2010).
629 9. J. R. Schramski, A. I. Dell, J. M. Grady, R. M. Sibly, J. H. Brown, Metabolic theory predicts
630 whole-ecosystem properties. *Proc. Natl. Acad. Sci. U.S.A.* **112**, 2617–2622 (2015).
631 10. P. B. Reich, M. G. Tjoelker, J. L. Machado, J. Oleksyn, Universal scaling of respiratory
632 metabolism, size and nitrogen in plants. *Nature* **439**, 457–461 (2006).
633 11. H. C. Muller-Landau et al. Testing metabolic ecology theory for allometric scaling of tree
634 size, growth and mortality in tropical forests. *Ecol. Lett.* **9**, 575–588 (2006).
635 12. D. A. Coomes, Challenges to the generality of WBE theory. *Trends Ecol. Evol.* **21**, 593–
636 596 (2006).
637 13. V. M. Savage, E. J. Deeds, W. Fontana, Sizing up allometric scaling theory. *PLoS Comput.*
638 *Biol.* **4**, e1000171 (2008).
639 14. F. Taubert, M. W. Jahn, H. J. Dobner, T. Wiegand, A. Huth, The structure of tropical
640 forests and sphere packings. *Proc. Natl. Acad. Sci. U.S.A.* **112**, 15125–15129 (2015).
641 15. J. A. Lutz et al. Global importance of large-diameter trees. *Glob. Ecol. Biogeogr.* **27**, 849–
642 864 (2018).
643 16. D. A. Coomes, E. R. Lines, R. B. Allen, Moving on from Metabolic Scaling Theory:
644 Hierarchical models of tree growth and asymmetric competition for light. *J. Ecol.* **99**, 748–756
645 (2011).
646 17. N. Picard, E. Rutishauser, P. Ploton, A. Ngomanda, M. Henry, Should tree biomass
647 allometry be restricted to power models? *For. Ecol. Manage.* **353**, 156–163 (2015).

18. T. L. Swetnam, C. D. O'Connor, A. M. Lynch, Tree morphologic plasticity explains deviation from Metabolic Scaling Theory in semi-arid conifer forests, Southwestern USA. *PLoS One* **11**, 1–16 (2016).

19. T. Jucker, et al. Allometric equations for integrating remote sensing imagery into forest monitoring programmes. *Glob. Chang. Biol.* **23**, 177–190 (2017).

20. K. J. Niklas, Size-dependent allometry of tree height, diameter and trunk-taper. *Ann. Bot.* **75**, 217–227(1995).

21. H. C. Muller-Landau, et al. Comparing tropical forest tree size distributions with the predictions of metabolic ecology and equilibrium models. *Ecol. Lett.* **9**, 589–602 (2006).

22. L. Banin, et al. What controls tropical forest architecture? Testing environmental, structural and floristic drivers. *Glob. Ecol. Biogeogr.* **21**, 1179–1190 (2012).

23. R. Aabeyir, S. Adu-Bredu, W. A. Agyare, M. J. C. Weir, Allometric models for estimating aboveground biomass in the tropical woodlands of Ghana, West Africa. *For. Ecosyst.* **7**, 7–41 (2020).

24. D. Zianis, M. Mencuccini, On simplifying allometric analyses of forest biomass. *For. Ecol. Manage.* **187**, 311–332 (2004).

25. D. Zianis, P. Muukkonen, R. Mäkipää, M. Mencuccini, Biomass and stem volume equations for tree species in Europe Silva Fenn. *Europ. J. Forest Res.* **4**, 1–63 (2005).

26. D. C. Chojnacky, Linda S. Heath, Jennifer C. Jenkins, Updated generalized biomass equations for North American tree species. *Forestry* **87**, 129–151 (2014).

27. J. Chave, et al. Improved allometric models to estimate the aboveground biomass of tropical trees. *Glob. Chang. Biol.* **20**, 3177–3190 (2014).

28. R. I. Barbosa, P. N. Ramírez-Narváez, P. M. Fearnside, C. Darwin, A. Villacorta, L. Camila, Allometric models to estimate tree height in northern Amazonian ecotone forests. *ACTA Amaz.* **49**, 81–90 (2019).

673 29. R. Valbuena, J. Heiskanen, E. Aynekulu, S. Pitkänen, P. Packalen, Sensitivity of above-
674 ground biomass estimates to height-diameter modelling in mixed-species West African
675 woodlands. *PLoS One* **11**, 1–24 (2016).
676 30. T. R. Feldpausch, et al. Tree height integrated into pantropical forest biomass estimates.
677 *Biogeosciences* **9**, 3381–3403 (2012).
678 31. X. Zhou, M. Yang, Z. Liu, et al. Dynamic allometric scaling of tree biomass and size. *Nat.*
679 *Plants* **7**, 42–49 (2021).
680 32. D. A. King, Linking tree form, allocation and growth with an allometrically explicit model.
681 *Ecol. Modell.* **185**, 77–91 (2005).
682 33. K. J. Niklas, Maximum plant height and the biophysical factors that limit it. *Tree Physiol*.
683 **27**, 433–440 (2007).
684 34. J. S. Sperry, F. C. Meinzer, K. A. McCulloh, Safety and efficiency conflicts in hydraulic
685 architecture: Scaling from tissues to trees. *Plant, Cell Environ*. **31**, 632–645 (2008).
686 35. J. N. Long, F. W. Smith, D. R. M. Scott, The role of Douglas-fir stem sapwood and
687 heartwood in the mechanical and physiological support of crowns and development of stem
688 form. *Can. J. For. Res.* **11**, 459–464 (1981).
689 36. Zhou, X., Yang, M., Liu, Z. et al. Dynamic allometric scaling of tree biomass and size. *Nat.*
690 *Plants* **7,** 42–49 (2021).
691 37. K. Ziemińska, D. W. Butler, S. M. Gleason, I. J. Wright, M. Westoby, Fibre wall and lumen
692 fractions drive wood density variation across 24 Australian angiosperms. *AoB Plants* **5**, 1–14
693 (2013).
694 38. A. E. Zanne, et al. Angiosperm wood structure: Global patterns in vessel anatomy and their
695 relation to wood density and potential conductivity. *Am. J. Bot.* **97**, 207–215 (2010).
696 39. J. S. Sperry, U. G. Hacke, J. Pittermann, Size and function in conifer tracheids and
697 angiosperm vessels. *Am. J. Bot.* **93**, 1490–1500 (2006).

698 40. T. A. McMahon, R. E. Kronauer, Tree structures: deducing the principle of mechanical
699 design. *J. Theor. Biol.* **59**, 443–466 (1976).
700 41. A. G. Greenhill, Determination of the greatest height consistent with stability that a vertical
701 pole or mast can be made, and of the greatest height to which a tree of given proportions can
702 grow. *Proc. Cambridge Philos. Soc.* **4**, 65–73 (1881).
703 42. K. A. McCulloh, J. S. Sperry, F. R. Adler, Water transport in plants obeys Murray's law.
704 *Nature* **421**, 939–942 (2003).
705 43. K. A. McCulloh, J. S. Sperry, F. R. Adler, Murray's law and the hydraulic vs mechanical
706 functioning of wood. *Funct. Ecol.* **18**, 931–938 (2004).
707 44. S. Patino, M. T. Tyree, E. A. Herre, Comparison of hydraulic architecture of woody plants
708 of differing phylogeny and growth form with special reference to freestanding and hemi-
709 epiphytic Ficus species from Panama. *New Phytol.* **129**, 125–134 (1995).
710 45. M. Larjavaara, H. C. Muller-Landau, Rethinking the value of high wood density. *Funct.*
711 *Ecol.* **24**, 701–705 (2010).
712 46. K. A. Preston, W. K. Cornwell, J. L. DeNoyer, Wood density and vessel traits as distinct
713 correlates of ecological strategy in 51 California coast range angiosperms. *New Phytol.* **170**,
714 807–818 (2006).
715 47. M. Fortin, R. Van Couwenberghe, V. Perez, C. Piedallu, Evidence of climate effects on the
716 height-diameter relationships of tree species. *Ann. For. Sci.* **76**, 1 (2019).
717 48. S. C. Stark, L. P. Bentley, B. J. Enquist, Response to Coomes & Allen (2009)'Testing the
718 metabolic scaling theory of tree growth'. *J. Ecol*. **99**, 741–747 (2011).
719 49. L. Poorter, D. M. A. Rozendaal, Leaf size and leaf display of thirty-eight tropical tree
720 species. *Oecologia* **158**, 35–46 (2008).

Supplementary Information.

Title: The Generalized Plant Allometry that Advances Metabolic Ecology Theory.

Authors: S.B.D. Sopp (1)*, and R. Valbuena (1)*

Affiliations:

(1) School of Natural Sciences, Bangor University, Bangor, LL57 2UW, UK

* **Corresponding authors:** s.sopp@bangor.ac.uk, r.valbuena@bangor.ac.uk

This file includes:

Supplementary figure (1)

Supplementary tables (1 and 2)

Supplementary figures

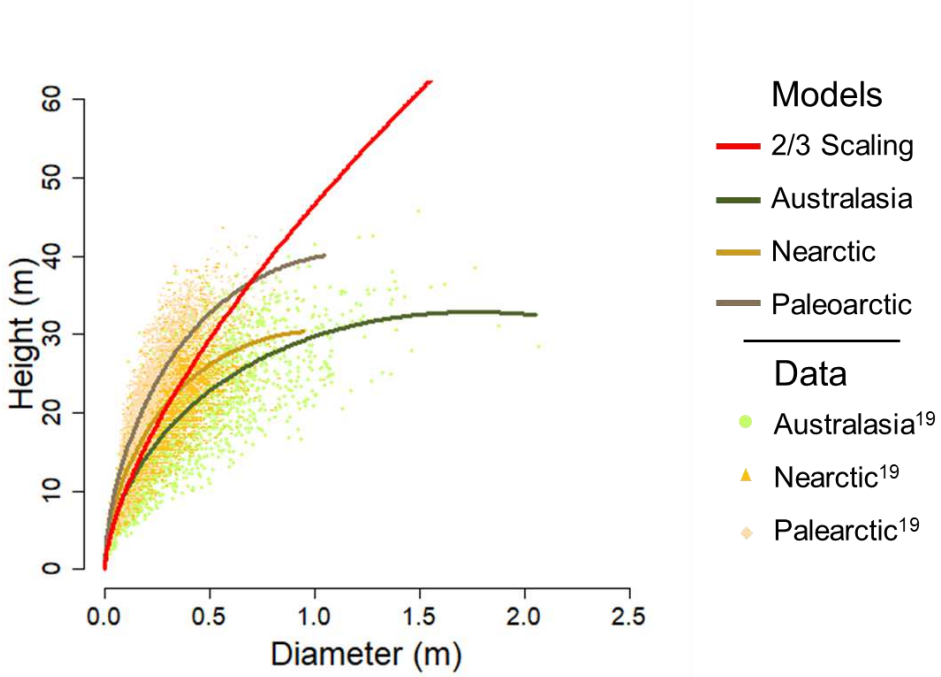

Supplementary Fig. 1 | Temperate mixed forest stratified by biome. Comparisons of height-diameter h-d models against the $2/3$ scaling rule: results for biogeographic regions for angiosperms in temperate mixed forests.

Supplementary Tables

Supplementary Table 1 | Summary tree height (*h*-*d*) models adjusted by NLS method (similar to Table 1 with MLE method).

Model	No. Observations	Coefficient Estimates $\widehat{\beta}_1$ (SE)	$\widehat{\beta}_2$ (SE)	Model Evaluation R^2	RMSD (%)	MD (%)
Chave *et al.*[27] data						
2/3 Scaling	4,004	44.2 (0.211)	-	0.73	5.59 (34.9)	-0.307 (-1.913)
Chave *et al.*[27] model (with $\boldsymbol{E}$)	4,004	-	-	0.87	3.82 (23.8)	-0.393 (-2.448)
gMET (with $\boldsymbol{E}$)	4,004	66.7 (0.524)	0.530 (0.008)	0.88	3.80 (23.7)	-0.065 (-0.406)
gMET (without $\boldsymbol{E}$)	4,004	52.0 (0.778)	0.276 (0.021)	0.74	5.52 (34.4)	0.109 (0.679)
Jucker *et al.*[19] data						
2/3 Scaling	79,335	46.5 (0.047)	-	0.70	5.00 (31.4)	-0.325 (-2.042)
Whole dataset	79,335	59.6 (0.181)	0.433 (0.004)	0.72	4.86 (30.5)	0.157 (0.990)
Gymnosperms		50.9 (0.397)	0.183 (0.014)	0.75	4.32 (25.6)	0.154 (0.913)
Boreal	4,942	45.2 (1.152)	0.006 (0.065)$^{n.s}$	0.63	2.97 (22.4)	0.026 (0.196)
Temperate Coniferous	9,539	48.7 (0.567)	0.038 (0.023)$^{n.s}$	0.83	4.06 (22.6)	0.131 (0.726)
Temperate Mixed	3,419	69.5 (0.730)	0.587 (0.012)	0.63	5.03 (24.8)	0.218 (1.073)
W&S	1,058	40.4 (1.572)	0.419 (0.061)	0.59	3.29 (26.2)	0.072 (0.572)
Angiosperm		61.5 (0.205)	0.474 (0.004)	0.71	5.00 (32.1)	0.156 (1.000)
Boreal	546	74.9 (2.595)	0.494 (0.066)	0.79	1.91 (10.8)	0.031 (0.174)
Temperate Coniferous	3,366	62.8 (1.062)	0.386 (0.029)	0.76	4.01 (25.1)	0.072 (0.452)
Tropical	32,251	65.1 (0.253)	0.482 (0.005)	0.77	4.84 (29.4)	0.118 (0.713)
W&S	10,591	38.5 (0.758)	0.217 (0.043)	0.50	4.33 (49.8)	0.124 (1.420)
Temperate Mixed						
Australasia	2,493	56.8 (0.706)	0.621 (0.010)	0.77	4.29 (26.8)	0.091 (0.569)
Paleartic	8,007	89.1 (0.799)	0.701 (0.010)	0.67	3.33 (18.2)	0.033 (0.180)
Neoartic	3,122	74.7 (0.512)	0.740 (0.007)	0.79	3.69 (17.2)	0.148 (0.689)

NLS: non-linear least squares. MLE: maximum likelihood estimation. gMET: generalized metabolic ecology theory model (Eq. 1). E: environmental stress parameter[2]. W&S: woodland and savannas. SE: standard error of coefficient estimate. R^2: coefficient of

744 determination. RMSD: root mean squared differences (in meters, and percentage of observed mean). MD: mean differences (in
745 meters, and percentage of observed mean). n.s.: non-significant β estimate (otherwise significant at 95% level at least).

746

Supplementary Table 2 | Stratum-wise comparison of 2/3 scaling rule against gMET *h-d* models adjusted by NLS.

	2/3 Scaling			gMET			ANOVA	
Model	**R^2**	**RMSD (%)**	**MD (%)**	**R^2**	**RMSD (%)**	**MD (%)**	**F value**	**P value**
Gymnosperms	0.75	4.33 (25.7)	0.029 (0.175)	0.75	4.32 (25.6)	0.154 (0.913)	117.3	< 0.0001
Boreal	0.63	2.97 (22.4)	0.025 (0.188)	0.63	2.97 (22.4)	0.026 (0.196)	0.0087	0.9254 n.s.
Temperate Coniferous	0.83	4.06 (22.6)	0.105 (0.585)	0.83	4.06 (22.6)	0.131 (0.726)	2.442	0.1181 n.s
Temperate Mixed	0.56	5.50 (27.1)	-0.475 (-2.335)	0.63	5.03 (24.8)	0.218 (1.073)	7,167	< 0.0001
W&S	0.58	3.33 (26.5)	-0.077 (-0.612)	0.59	3.29 (26.2)	0.072 (0.572)	23.52	$1.421 \cdot 10^{-06}$
Angiosperm	0.69	5.20 (33.3)	-0.436 (-2.795)	0.71	5.00 (32.1)	0.156 (1.000)	4,842	< 0.0001
Boreal	0.77	1.96 (11.03)	-0.060 (-0.340)	0.79	1.91 (10.8)	0.031 (0.174)	28.58	< 0.0001
Temperate Coniferous	0.75	4.07 (25.49)	-0.207 (-1.293)	0.76	4.01 (25.1)	0.072 (0.452)	100.1	< 0.0001
Tropical	0.74	5.13 (31.1)	-0.631 (-3.828)	0.77	4.84 (29.4)	0.118 (0.713)	4,003	< 0.0001
W&S	0.50	4.33 (49.8)	0.0517 (0.594)	0.50	4.33 (49.8)	0.124 (1.420)	18.44	$1.770 \cdot 10^{-05}$
Temperate Mixed								
Australasia	0.70	4.96 (30.9)	-0.968 (-6.03)	0.77	4.29 (26.8)	0.091 (0.569)	828.8	< 0.0001
Paleartic	0.56	3.80 (20.8)	-0.534 (-2.92)	0.67	3.33 (18.2)	0.033 (0.180)	2,447	< 0.0001
Neoartic	0.70	4.41 (20.5)	-0.702 (-3.26)	0.79	3.69 (17.2)	0.148 (0.689)	1,332	< 0.0001

NLS: non-linear least squares. W&S: woodland and savannas. R^2: coefficient of determination. RMSD: root mean squared differences (in meters, and percentage of observed mean). MD: mean differences (in meters, and percentage of observed mean.

750

45

Figures

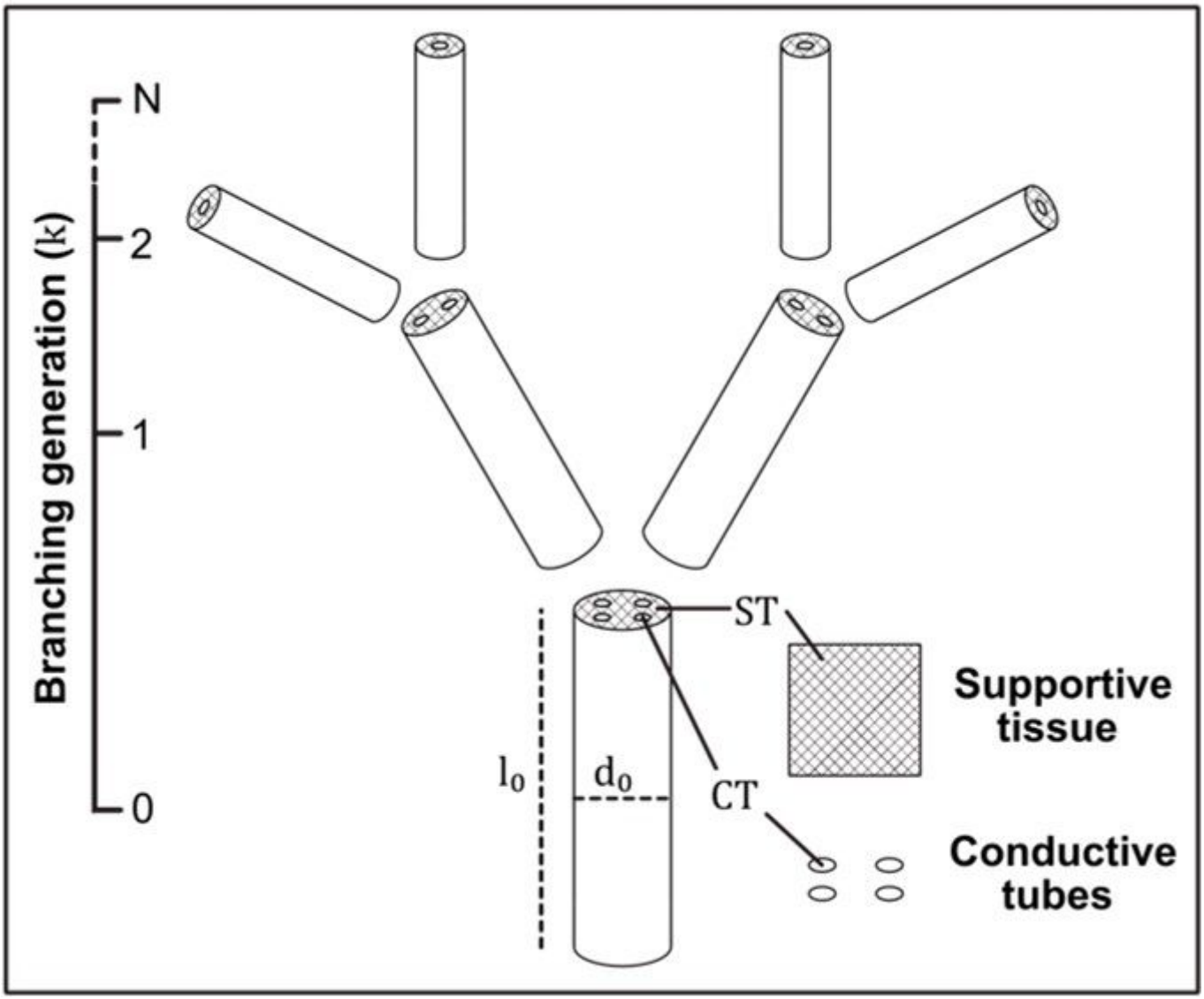

Figure 1

Tree architecture illustrating the differentiation of supportive and conductive systems within a branching network. This differentiation is set out by Eq. 9.

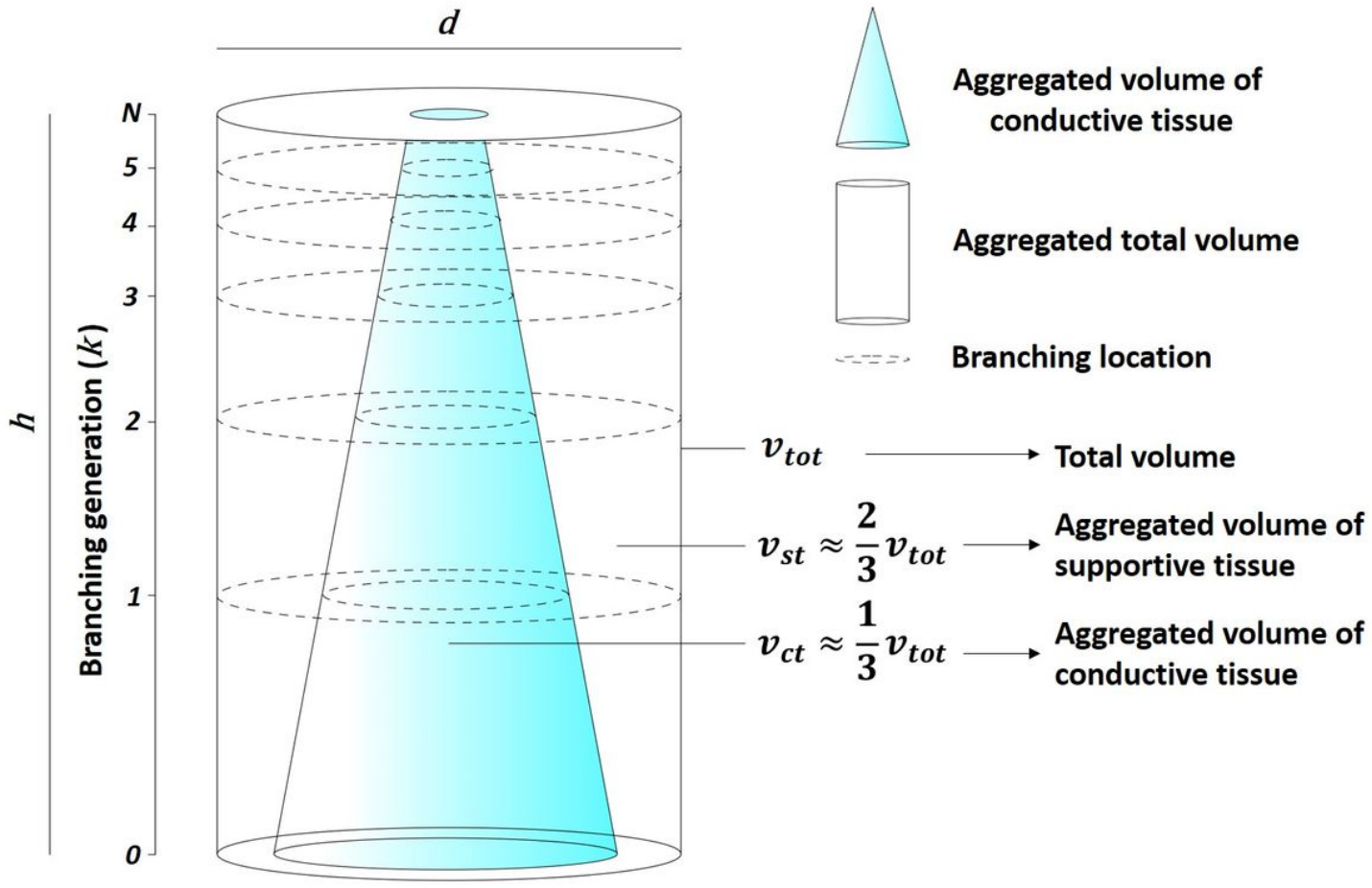

Figure 2

Truncated Cone & Cylinder approximation of tree volumes. This visualization illustrates the modelization of aggregated volumes of conductive tissues across branching generations (blue cone) within the total volume (cylinder).

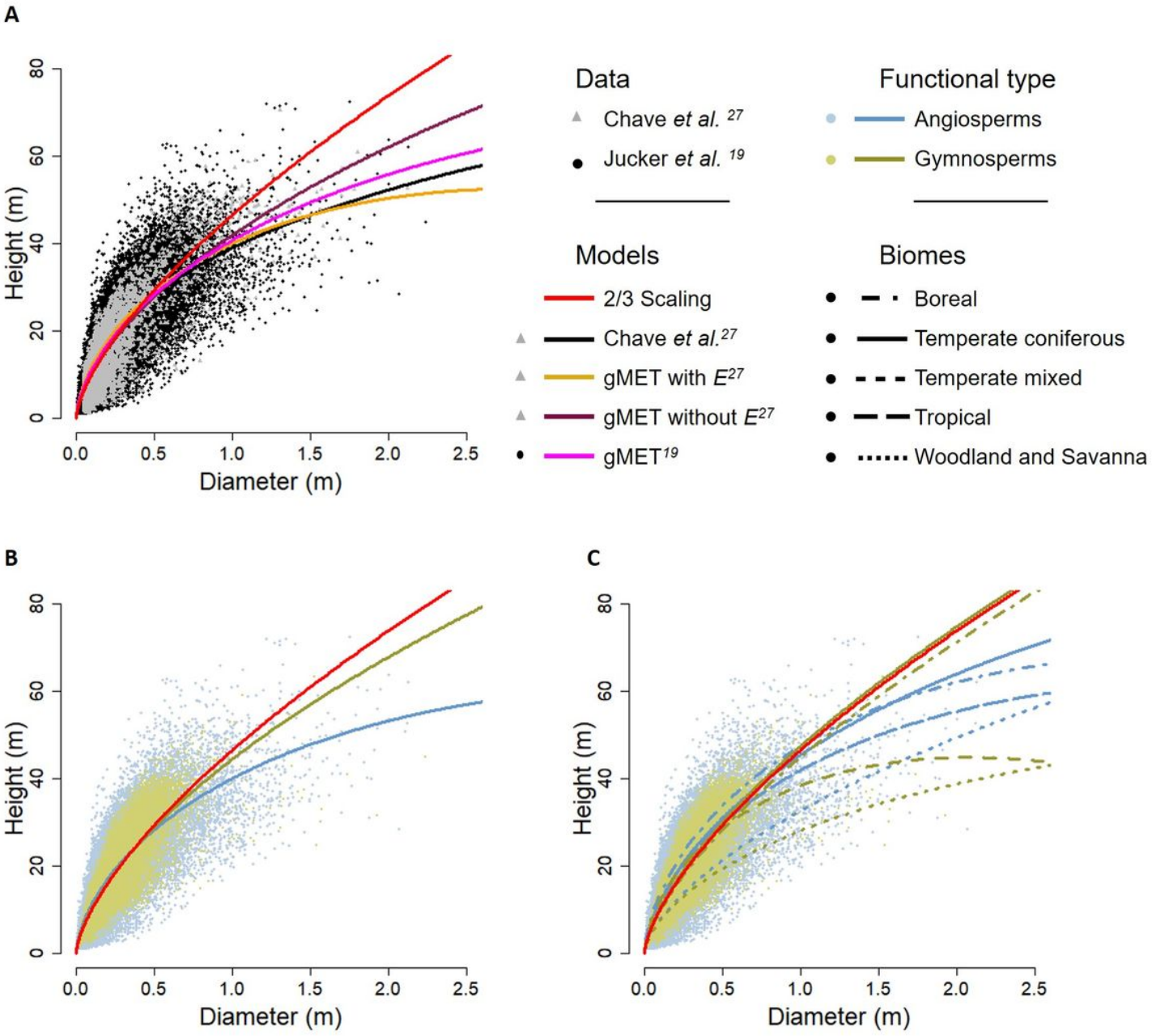

Figure 3

Height-diameter model results. Comparisons of height-diameter □-□ models against the 2/3 scaling rule (in red). (A) Our generalized metabolic ecology theory (gMET) model for □ (Eq. 1) adjusted to empirical data from either Chave et al. 27 (grey triangles) or Jucker et al. 19 (black dots), also comparing against Chave et al.'s □-□ quadratic log-log model27. (B) gMET □-□ models adjusted by functional group (sensu Jucker et al. 19): gymnosperms versus angiosperms. (C) gMET □-□ models adjusted by functional group / biome combination19. □: environmental stress parameter27 .

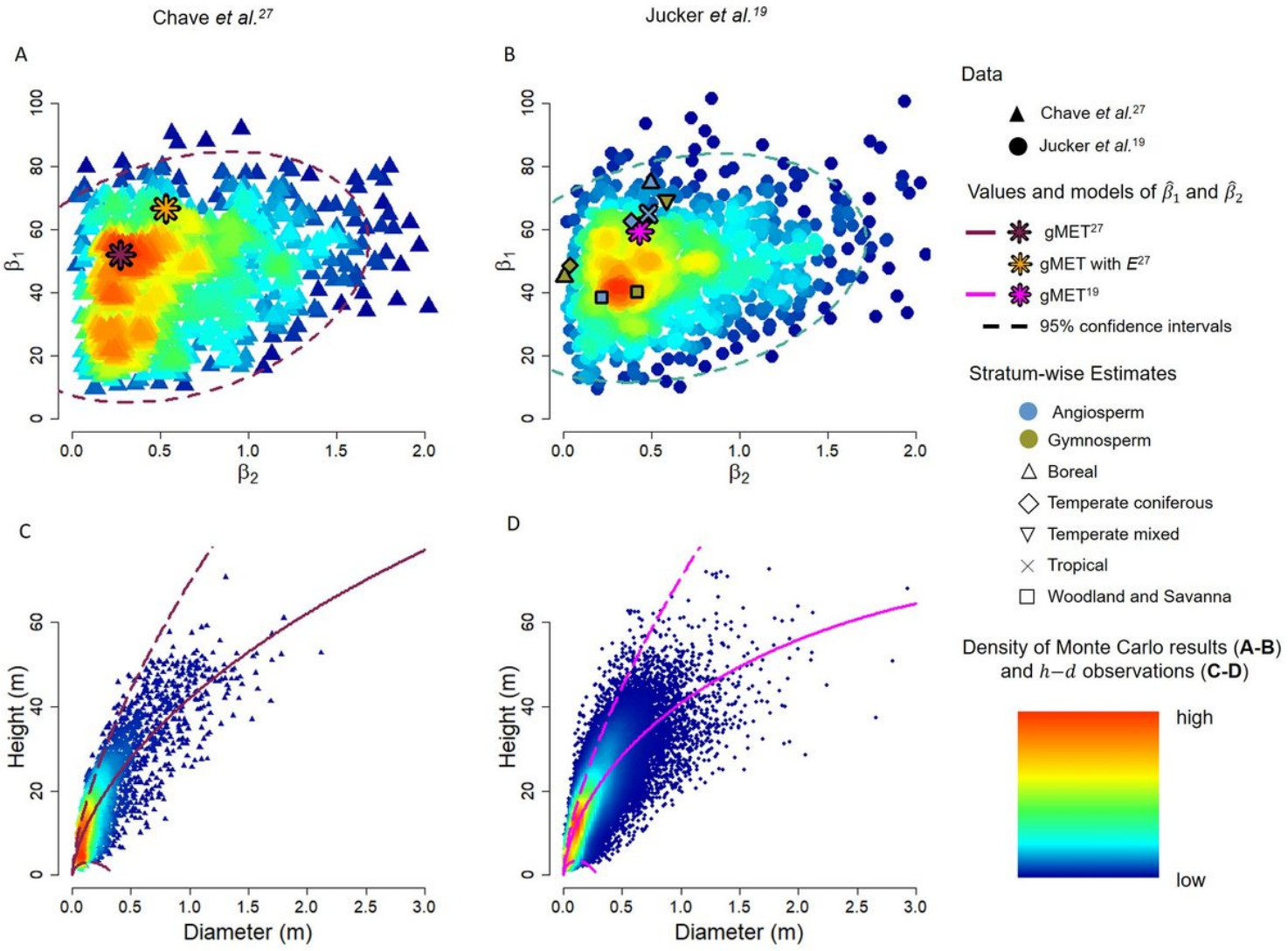

Figure 4

Monte Carlo results, and their confidence intervals propagated on height diameter models. Monte Carlo simulations compared against estimated 1 and 2 values. (A-B) Density plots of 1-2 join distributions generated through Monte Carlo simulations, for both pantropical27 (A) and global19 (B) datasets, with 95% confidence intervals given obtained through a 2 distribution. (C-D) Monte Carlo simulation-derived 95% confidence interval values for 1 and 2, propagated into the - gMET (without) model

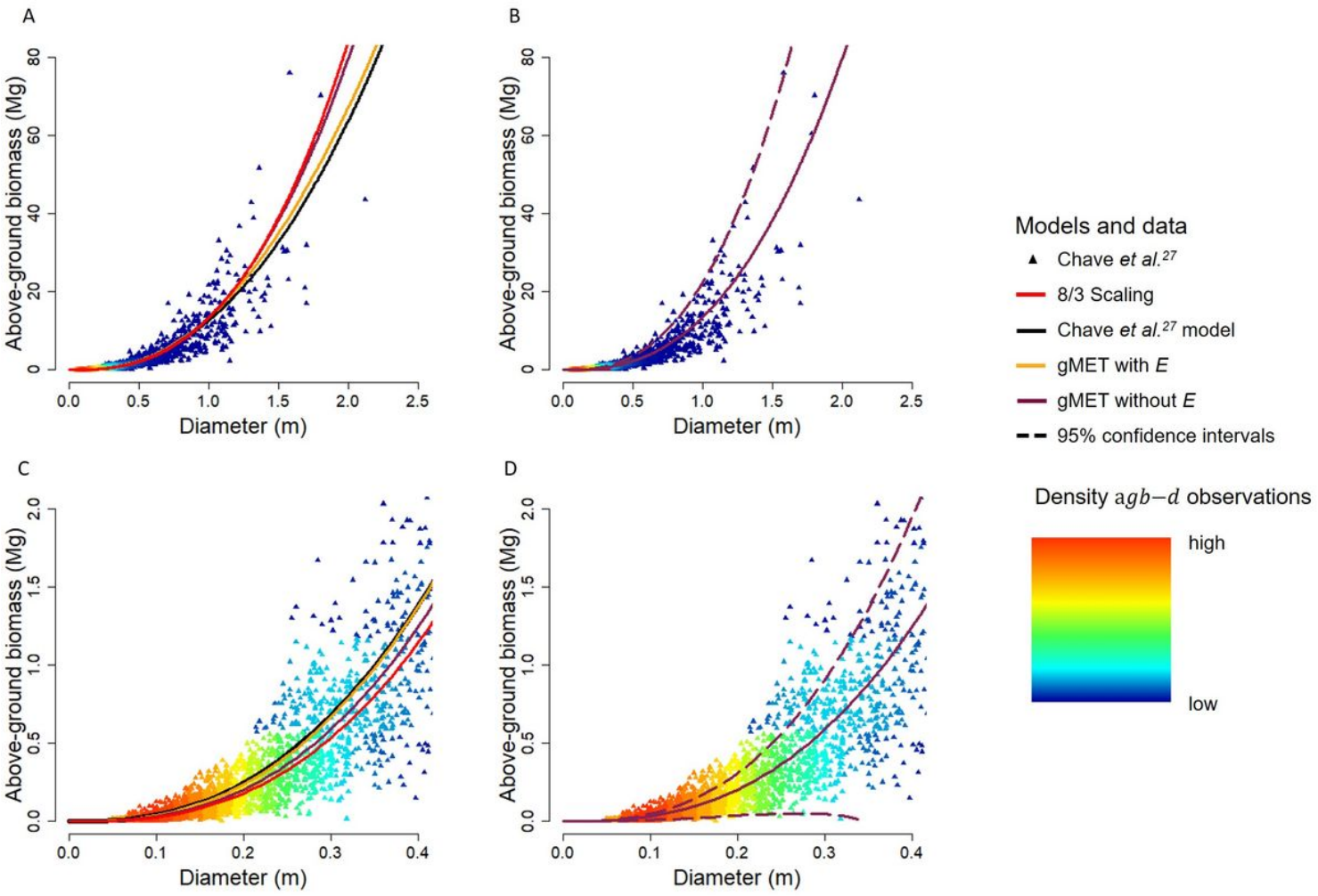

Figure 5

Above-ground biomass-diameter model results. Comparisons of biomass-diameter □□□-□ models against the 8/3 scaling rule (in red). (A) Our generalized metabolic ecology theory (gMET) model for □□□ (Eq. 3) adjusted to empirical data from Chave et al.27 is presented (with and without □), compared against Chave et al.'s27 □□□-□ quadratic log-log model. □: environmental stress parameter27. (B) Monte Carlo simulation-derived 95% confidence interval values for □1 and □2 (Fig. 2C), propagated into the □□□-□ gMET (without □) model. (C-D) enhancements of panels A and B showing only the data for smaller trees.

Supplementary Files

This is a list of supplementary files associated with this preprint. Click to download.

- suppFig1BiogeographicZones.jpg